A NEW METHOD FOR GENERATING SHORT OPTICAL PULSES

by

Steve J. Shattil

A thesis submitted to the Faculty and the Board of Trustees of the Colorado School of Mines in partial fulfillment of the requirements for the degree of Master of Science (Physics).

Golden, Colorado

date 11/20/87

Signed: Steve J. Shattil

Approved: Dr. Frank V. Kowalski
Thesis Advisor

Golden, Colorado

Date 12/10/87

Dr. John U. Trefny
Professor and Head,
Physics Department

ABSTRACT

A novel laser is built which produces picosecond pulses and pulse bursts in which the pulses are seperated by only a few picoseconds; a repetition rate that is not matched by any other laser.

An acousto-optic modulator (AOM) shifts the frequency of light inside the cavity of a dye laser by an amount equal to the mode spacing of the cavity (the speed of light divided by the cavity length). The frequency-shifted light is then fed back into the gain medium. The gain medium is R6G dye pumped by an argon- ion laser. Inserting a frequency selective element into this cavity produces short optical pulses. Pulse-broadening is observed when either the cavity length or modulation frequency is deviated slightly from the condition for which optimal pulsing occurs, and multiple pulses are observed when the deviations are more significant. Finally, computer modelling is used to reproduce and thus support our observations of pulse-broadening and multiple pulse production.

TABLE OF CONTENTS

LIST OF FIGURES AND TABLES

ACKNOWLEDGMENTS

I wish to thank Paul Hale and Brad Cohen for helping me solve the many problems I encountered while writing and revising the computer programs I used in my research. It should be noted that Jack Kinter provided expert counsel and valued services in machining many components that were essential to the construction of our laser. Yosi Neev provided much assistance in using the dye laser. Most of all, I wish to thank Dr. Frank Kowalski. Without his help and guidance, this project would not have been possible.

I INTRODUCTION

A laser output having a high repetition rate of short optical pulses (less than 20 psec.) has numerous applications. These include investigations of ultra-fast phenomena, research in nonlinear optics, spectroscopy, and optical information processing.

Synchronous pumping of dye lasers is the most reliable technique known for generating ultra-short optical pulses. In the synchronous pumping process, the output pulses of a mode-locked ion laser are used to excite a dye laser whose cavity has been extended such that the intermode frequency spacing is an integral multiple of the mode locker frequency. In this case, the dye laser is mode-locked by external means.

Our objective was to build a pulsed laser by mode-locking a dye laser internally. The designing and building of this device were performed under the direction of Dr. Frank Kowalski. The result is that our laser is more stable, and it produces shorter pulses at a much higher repetition rate than a synchronously-pumped mode-locked dye laser system. Our system will also be significantly less expensive to reproduce than the commercial synchronously pumped systems.

Mode-locking is the principle of adding together harmonic waves of different frequencies having a fixed phase relationship between them, and results in the production of very short pulses occurring at a high repetitive rate. In our laser, this locking is achieved by internal means; that is, an AOM is located inside the laser cavity. The light inside the cavity is stepped up in frequency each time it passes through the AOM. Pulses are generated when the modulation frequency is an integral multiple of the mode spacing (1).

The effect of the AOM on the spectral content of the laser was determined using a spectrograph and a variable length interferometer. The results are that the laser produces a broad band spectrum with a bandwidth of about 6 angstroms.

Mode-locking occurs when there are restrictions imposed on the allowed frequencies of light oscillating in the laser cavity: Pulses are observed when the laser is operating near threshold, or when a frequency selective device is inserted into the cavity.

A fast photo-detector and an autocorrelator were used to detect and measure the pulses. Variations in pulse shape and height are discussed with respect to changes made in the cavity length and the modulator frequency. Our observations are then compared to the results from computer programs which simulate mode-locking and auto-correlations.

II APPARATUS

The argon laser beam is directed onto the dye jet by the pump mirror m(p). Mirrors m1, m2, m3 , and m4 form the cavity of the dye laser (figure 1). The mirror seperations in cm are: m1 to m2 8.5, m2 to m3 34.5, m3 to m4 57, and m4 to m1 34.

The dye is pumped at a pressure of about 90 psi. The dye jet is at Brewster's angle to avoid reflection losses at the surface of the jet.

The astigmatism compensator is located between m2 and the dye jet. It is a fused silica rhomb which compensates for astigmatism caused by the dye jet and regions of the beam inside the cavity which are off-axis at the curved mirrors.

The AOM (Isomet Model 1211) operates from 100 to 120 MHz and is driven by a synthesized source. The modulator is located between mirrors m3 and m4 a distance of 29.5 cm from m4 and can be rotated about an axis perpendicular to the plane of figure 1. The laser operates either bidirectionally, or in a clockwise traveling wave or counterclockwise traveling wave depending on a slight adjustment of this rotation angle.

Light passing through the AOM is diffracted through planar acoustical waves in the modulator crystal. The efficiency of our AOM in diffracting light into the first order is 90% for a modulator amplitude of 90 mV and frequency of 110 MHz. Light diffracted into the first order remains inside the cavity and the zeroth-order diffracted light is the output beam.

The output beam was directed into a Model 70-000, 3.4 meter Jarrell-Ash spectrograph for the frequency spectrum analysis. For the pulse analysis and measurements, the beam was split into two parts: One beam was monitored by a fast photo-detector and an oscilloscope having a rise time of about one nanosecond. The other beam was sent into an auto-correlator (Spectra Physics, model 409 with a range of 80 to .5 picoseconds).

In order for laser oscillation to occur, the gain of the medium must be greater than the sum of all the losses in the cavity. The gain of the dye increases linearly with the argon laser power until the point where the gain medium becomes saturated or thermal lensing occurs. We initiated lasing in our system by using a high argon laser power (about 4 watts), and we minimized losses by keeping the cavity mirrors free of dust, and reduced the effects of air currents by enclosing the system in a plexi-glass case. Lasing is optimized by adjusting the alignment of the cavity mirrors and the position of the argon laser beam on the dye jet.

Our laser uses mirrors of the same curvature as the Spectra Physics model 380D ring dye laser and initially had similar dimensions. We extended the length of the laser cavity from 124 cm to 135 cm. In order to extend the cavity, we needed to calculate the stability condition with respect to many different cavity alterations which yielded the desired cavity length. This was done using the computer program Cavity.par (appendix A), which calculated the ABCD matrix for any given optical cavity, the stability condition, and the waist size and radius of curvature at the start/end of the cavity.

The feedback cavity (figure 2) is about the same length as the primary cavity (135cm). The mirror mR is on an adjustable mount which allows us to vary the cavity length by almost 2.5 cm. Either of two mirrors was used between the main and feedback cavities (at m4). They were output couplers, one having 1% and the other having 10% transmittance.

FIGURE 1

Diagram of the Dye Laser Cavity

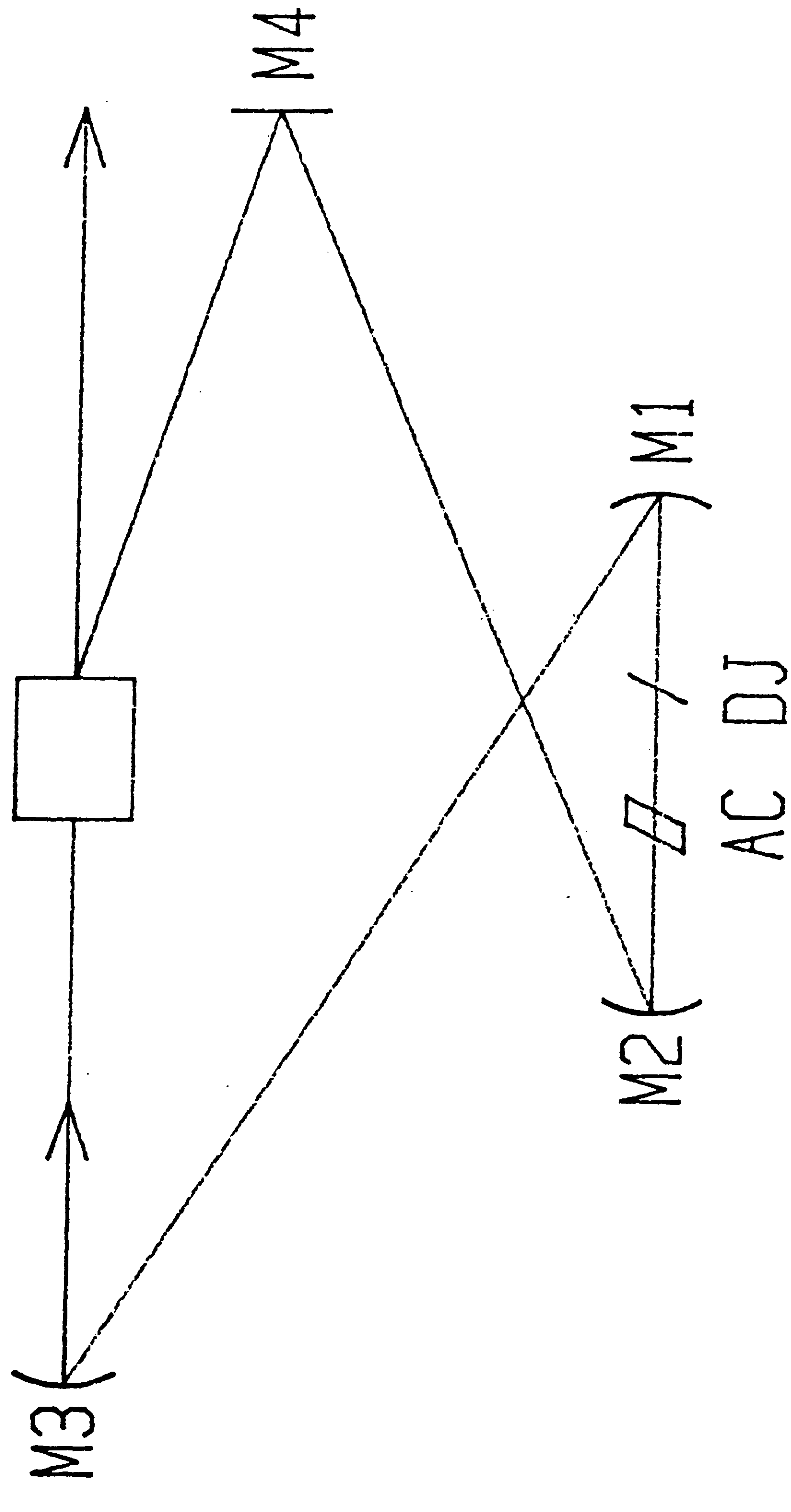

FIGURE 2

Dye Laser with Feedback Cavity Included

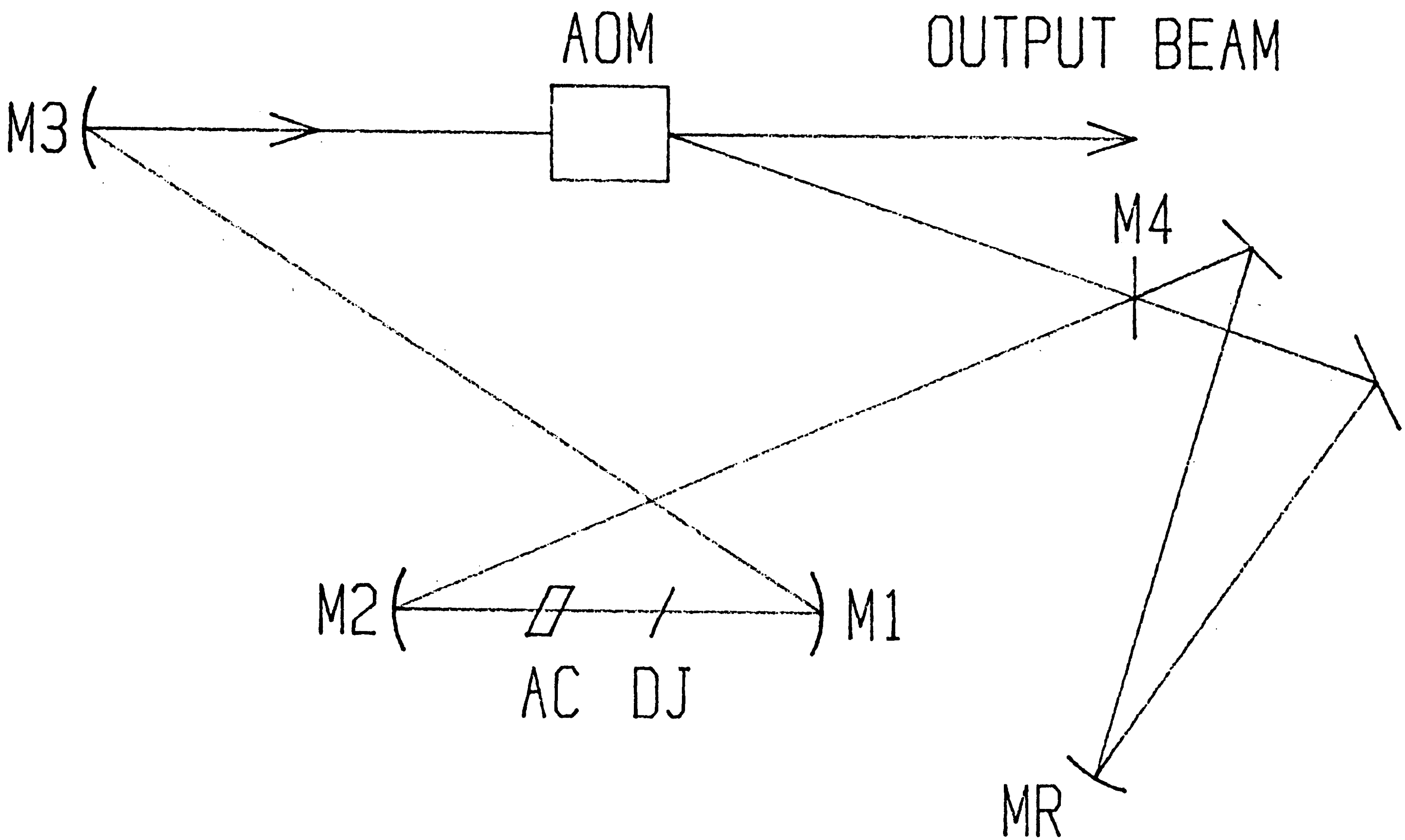

III FABRY-PEROT CAVITIES AND THE TRAVELING WAVE CAVITY

The standard method for sustaining laser oscillation is with feedback in a Fabry-Perot cavity (1). The multiple reflections within the cavity lead to destructive interference for all frequencies of light except those discreet frequencies which correspond to the standing waves of the cavity. This is demonstrated by the example of multiple-beam interference occurring within an etalon.

Let r be defined as the coefficient of reflection, and t be defined as the coefficient of transmission.
The amplitude of the initial ray is Eo.
The amplitude of that ray when it enters the etalon is Eot. Then for each time the ray is internally reflected it is multiplied by r: Eotr, Eotr, Eotr, . . .

The intensity of the transmitted light is (2)

$$I = |E|^2 = |E|^2|t|^4 \,/\, |1-r \exp(-iwd/c)|^2$$

which can be written

$$I = T^2 / \left[(1-R)^2 + 4R \sin^2(wd/c) \right]$$

$$\text{where } T = |t|^2 \text{ and } R = |r|^2$$

The intensity of the transmitted light is sharply peaked at the resonance of the cavity: $w = n\, c/d$

$$I(max) = IoT^2 / (1-R)^2$$

The antiresonance condition gives the minimum transmitted intensity:

$$I(min) = IoT^2 / (1+R)^2$$

Substituting the value .99 for R we find that I(max) is almost 40,000 times greater than I(min), which demonstrates how a Fabry-Perot cavity practically disallows fields which do not have a resonant frequency of the cavity.

Our system is a traveling wave laser, which is distinguished from a standing wave laser. A standing wave laser has two waves of equal amplitude traveling in opposite directions. The disadvantage of a standing wave dye laser is that boundary conditions require the maxima and minima of the wave in the cavity to be stationary. Thus the regions of the gain medium where minima of the intracavity radiation field are located are not stimulated by feedback radiation. This phenomenon, known as spatial hole-burning, limits the output power of a standing wave dye laser particularly when it is lasing in a single frequency.

A traveling wave dye laser (or ring dye laser) does not produce spatial hole burning because the waves circulate in only one direction around the cavity and thus uniformly saturate the gain medium. This laser can be made to operate in a single frequency by the appropriate combination of etalons which allow only a single mode to oscillate. Although a standing wave is established inside the etalon, we have a traveling wave outside the etalon because of the unidirectional nature of our laser. Unidirectionality is achieved by tilting the AOM, which in certain orientations causes substantially more loss for light traveling in one direction than the other.

IV CONTINUOUS WAVELENGTH CHARACTERISTICS

The dye laser is optically pumped by the argon laser beam. When a dye molecule absorbs a photon from the pump laser beam, it is excited to a higher energy level from which it decays. The energy levels are broadened by electrostatic perturbations and collisions with other molecules, particularly, solvent molecules, which are much smaller than the dye molecules. The resulting radiative process is a cascading effect which causes the emission spectra of the dye to be practically continuous.

Some of the photons produced by this spontaneous emission process leave the dye jet at such an angle that they remain inside the laser cavity and return to the dye jet. When the photons go through the dye a second time they cause stimulated emission. This process produces photons that have the same frequency as the initial photons and travel in the same direction. Thus the beam gains energy each time it passes through the dye jet (gain medium).

In our system, the broad-band spectrum of the spontaneously emitted light from the gain medium is frequency-shifted by the AOM before it returns to the gain medium. Thus we are not getting resonant frequency build-up as in a Fabry-Perot device. Rather, all frequencies of light in the cavity will have the same intensity, and light of different frequencies interfere to produce a beat of about 4.5 nanoseconds.

Analysis of the spectral content of the output beam was aided by a variable length interferometer and a Jarell-Ash spectrograph, which has a diffraction grating (590 grooves/mm) and was operated in the second order, giving a dispersion of 2.5 A/mm at the image plane of the spectrograph. Analysis was made when the laser was operating away from conditions in which pulses would be generated. No pulses were observed using the fast photo-detector or the autocorrelator. The bandwidth of the laser was measured to be approximately 6 A, and there was no indication of discrete frequencies in the fringe pattern of the spectrometer with a resolution of 14 MHz.

We determined that the AOM acts as a diffraction grating when we observed frequency tuning resulting from changing the angle at which light in the cavity enters the AOM. This is achieved by either readjusting the tilt of the AOM or changing the vertical angle of the mirrors m3 and m4 (figure 3). The AOM diffracts light in accordance to its wavelength and thus causes light that is not inside the 6 A bandwidth to transit out of the cavity. If the mirrors m3 and m4 were closer to the AOM, the bandwidth would be larger.

FIGURE 3

Diffraction of Light Through the AOM

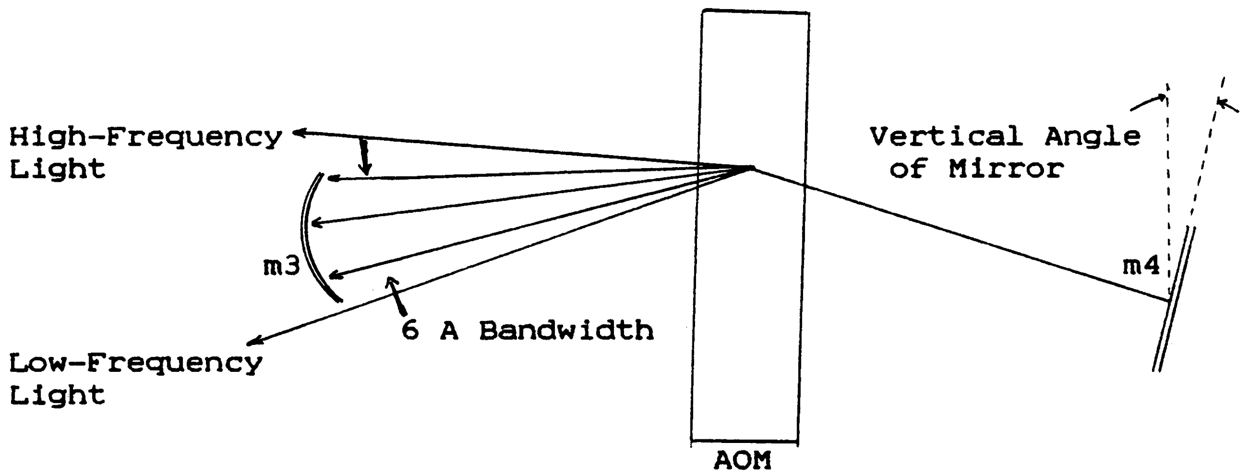

V OPTICAL PULSE PRODUCTION

If we consider the superposition of fields circulating in a passive cavity where there is an initial frequency, w, of light having an amplitude Eo, and it experiences a shift in frequency of Ω each time it passes through an AOM, then we get the following expression for the intensity (3):

$$I = Iot \,/\, [(1-r)^2 + 4r \sin^2(\Delta/2)]$$

where r is the amplitude reflection coefficient into the first order diffracted beam, t is the amplitude transmission coefficient into the zeroth order diffracted beam, L is the length of the cavity which is set such that $\Omega L/c = 2\pi$ (Ω is in radians per second), and $\Delta = wL/c + aL/c - \Omega\tau$. We note that the intensity as a function of Δ is identical to the Airy function which illustrated frequency discrimination in the Fabry-Perot cavity, except that Δ is time dependent. This function represents the production of pulses at a time interval of $\Delta\tau = 2\pi/\Omega$. Our device differs from the passive cavity which this analysis is based on in that it has a gain medium within the cavity. The importance of this analysis with respect to our laser is that we observe pulses when we use mechanisms to frequency limit our laser.

We observed pulses when our laser was operating near threshold. At threshold, the light in the cavity is probably frequency limited: There is substantially more loss for light of some frequencies than there is for others. We would expect that a Fabry-Perot feedback cavity, or an etalon would also frequency limit the light that will oscillate inside the laser cavity, and result in the production of pulses. We observed pulses when either of these devices were used, however we were unable to detect discrete frequencies of light at any time.

The free spectral range of our thin etalon was 900 GHz (or about 12 A). Because the bandwidth of our laser is 6 A, the etalon can select only one frequency. Light at this frequency circulates in the cavity and is shifted by 110 MHz for each pass through the AOM. We observed the largest single-pulse autocorrelation signal when we had the etalon in the cavity. However, we did not observe a multiple pulse signal as we did when we used the feedback cavity.

A Fabry-Perot feedback cavity is utilized when a 10% output coupler is used in place of the mirror m4 (see figure 2). The output beam is directed into the autocorrelator, which displays the amplitude and duration of the pulses by means of second harmonic generation. The path of the beam in the autocorrelator is shown in figure 4. The incoming beam is split into two beams inside the autocorrelator. The beams have a variable delay with respect to each other due to the passage of one beam through a rotating quartz block in one arm of the interferometer. The two beams cross inside a potassium dihydrogen phosphate (KDP) crystal. When the beam passes through the KDP crystal, second harmonic generation causes a reradiation of light that is twice the frequency of the incident light (4). The magnitude of second harmonic generation is proportional to the intensity of light inside the crystal, and thus is proportional to the degree of pulse overlap where the two beams cross.

The autocorrelation signal is particularly sensitive to the AOM frequency and the length of the feedback cavity. These two parameters are dependent on each other. For instance, we obtained an optimal autocorrelation spike, which we defined by the minimum full-width half-maximum of the spike, when the AOM frequency was 110.887 MHz and the setting for mR was .365 inch. When the AOM frequency was reduced to 110.865 MHz, the peak broadened, and it decreased in amplitude. Then we adjusted the position of mR until the initial signal was obtained. This occurred at the setting of .361 inch.

We observed that the autocorrelation spike broadened and decreased in amplitude when either the position of mR or the AOM frequency was deviated from the conditions which yielded the optimal signal. A single autocorrelation spike was present within the range of .01 inch about the mR setting corresponding to the optimal signal, and a 5 KHz range about the AOM frequency for that signal.

The autocorrelation signal is calibrated by an etalon, which is inserted into both beams in the autocorrelator and results in a shift in the signal by 40 picoseconds (psec). We found that each division on the oscilloscope corresponds to 15.4 psec on the normal scale, and 1.54 psec on the expanded (10X) scale. Figure 5 shows a single peak autocorrelation signal which has a full width, half max of 4 boxes at 1.54 psec/box. Dividing this full width, half max by 2 gives the full width, half max of the pulses in the beam entering the autocorrelator, which is 3.1 psec.

When either the AOM frequency or the setting for mR is deviated beyond the parameters where the single pulse disappears, we observed multiple spikes in the autocorrelation signal (figure 6). These spikes had smaller amplitudes than the single spike signal. As the AOM frequency and mR setting were deviated even more, the signal appears to spread out. The space between the spikes increases, but the number of spikes in the signal decreases (figures 7 and 8).

FIGURE 4

Beam Path in the Autocorrelator

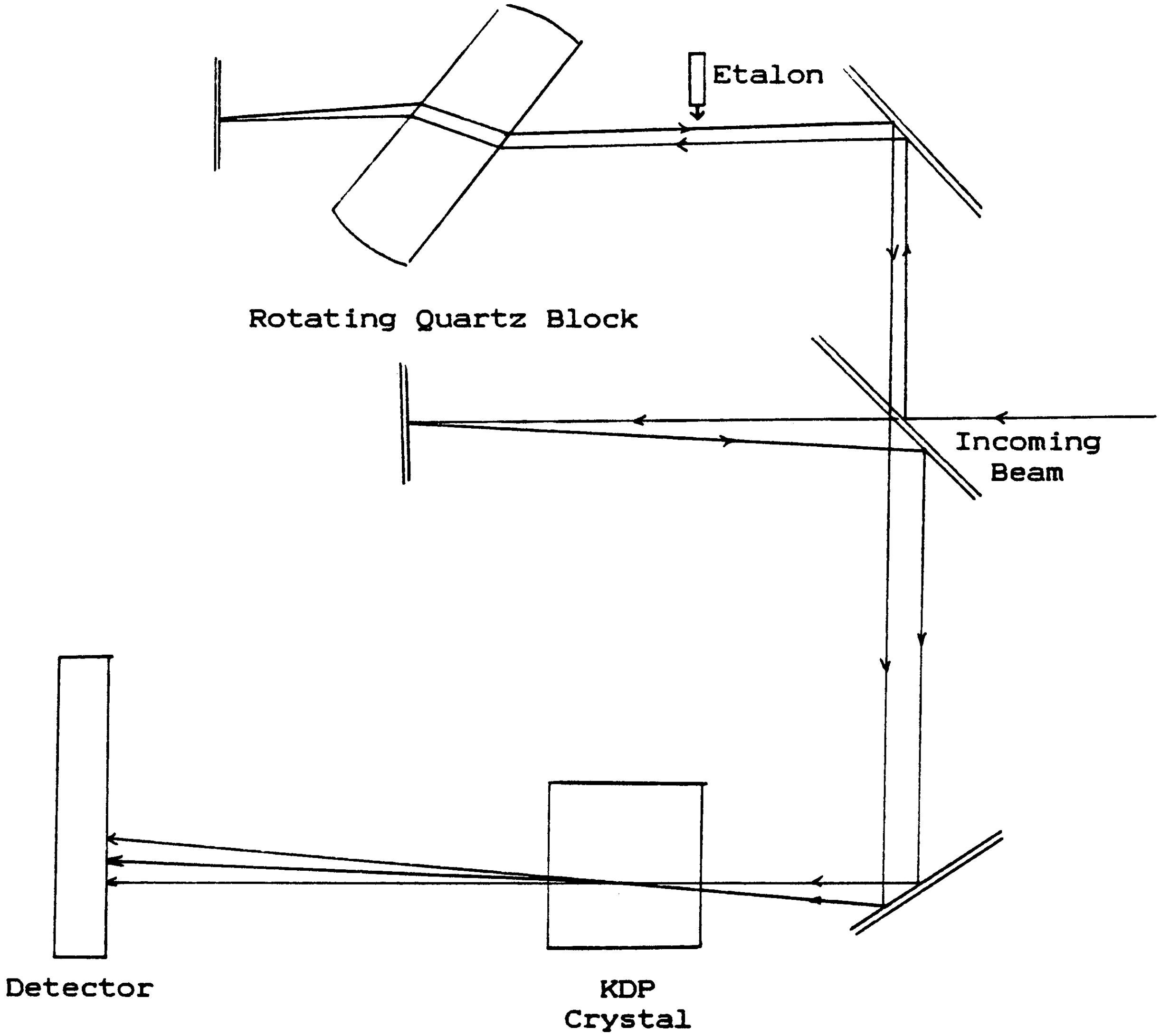

One arm of the autocorrelator varies in length (due to the rotating quartz block) and results in a variable time delay for the beam traveling in that arm. An etalon can also be inserted in that arm to cause a 20 or 40 psec time delay depending on whether it is inserted in one or both beams. This is done for the purpose of calibration.

FIGURE 5

Single Spike Autocorrelation Trace

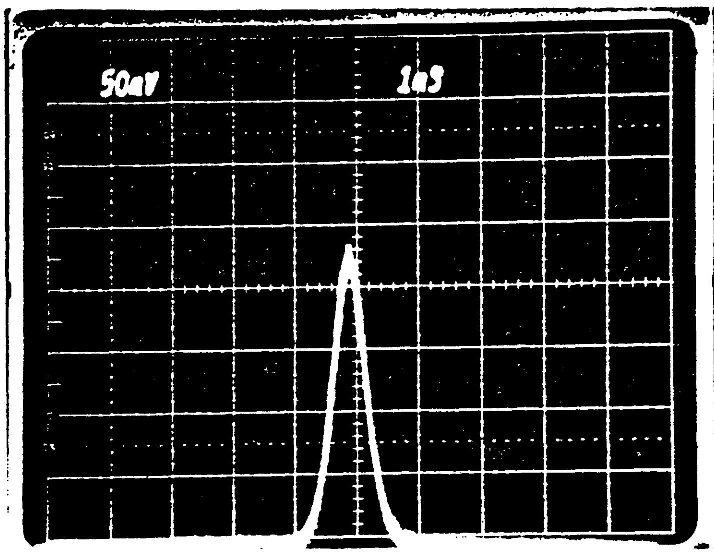

FIGURE 6

Multiple Spike Autocorrelation Trace
Mirror mR setting of .361 inches

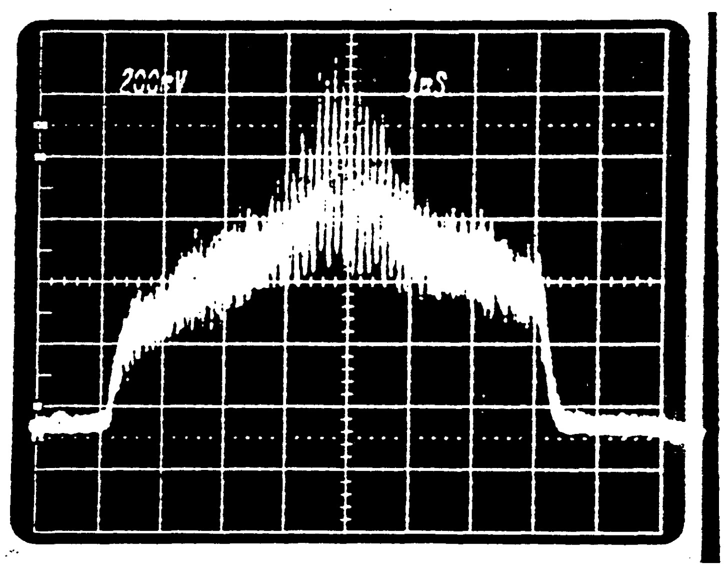

FIGURE 7

Multiple Spike Characteristics Relative to an Increase in Length of the Feedback Cavity

a. Mirror mR setting of .354

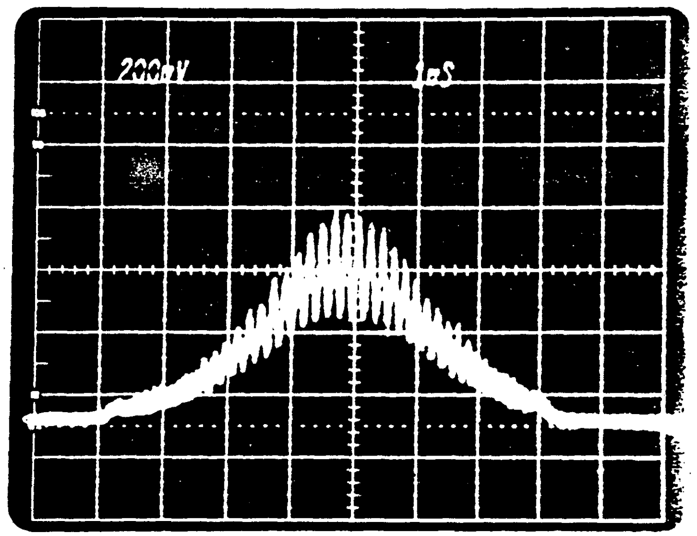

b. Mirror mR setting of .347

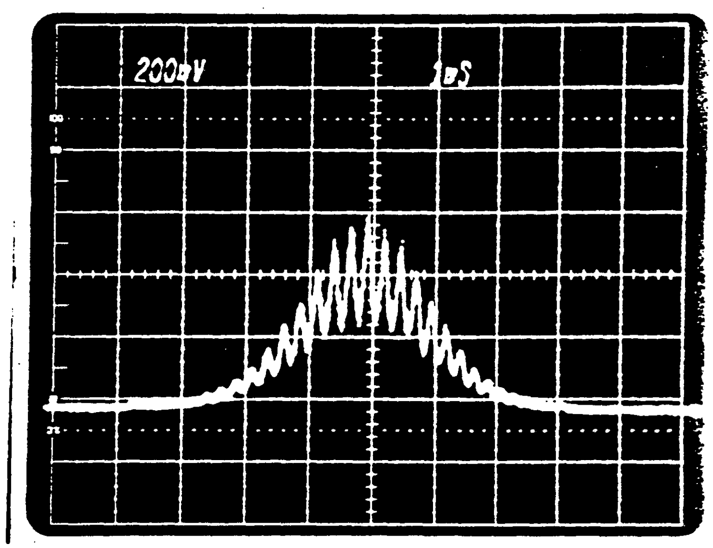

FIGURE 8

Multiple Spike Characteristics Due to Further Increases of the Feedback Cavity Length

a. Mirror mR setting of .345

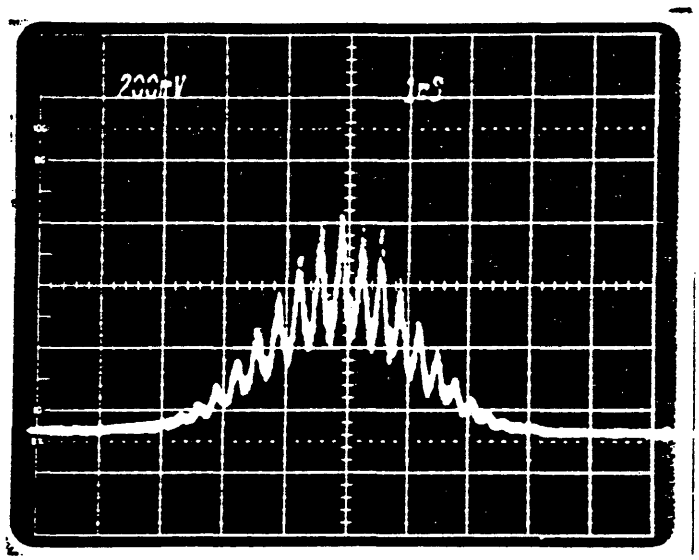

b. Mirror mR setting of .335

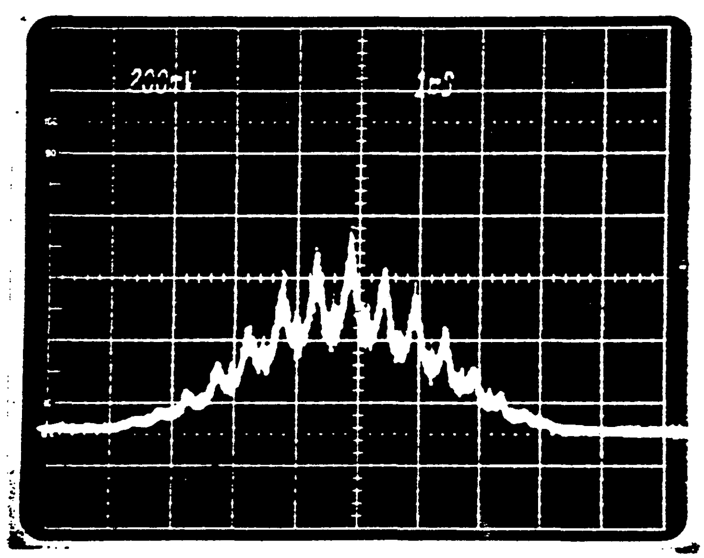

VI COMPUTER ANALYSIS OF THE AUTOCORRELATION FUNCTION

We hypothesized that the phenomenon of multiple spikes occurring in the autocorrelation signal was due to there being more than one pulse inside the interferometer at one time. The frequency of spikes occurring in the autocorrelation signal is equivalent to the frequency of pulses in the laser beam. The number of spikes in the autocorrelation signal is 2n-1, where n is the number of pulses in one arm of the interferometer.

We used the computer program TEST.PDH (appendix B) to perform the autocorrelation function for a given series of gaussian- shaped pulses. One will note the similarity between the computer-generated autocorrelation signal (figure 9) and the observed signals in figures 7 and 8. This close resemblance was unexpected due to the fact that the computer-generated signal was produced from a finite train of pulses (figure 10). We had anticipated that the observed autocorrelation signal was the result of an infinite train of pulses.

In order to test the assumption that the observed autocorrelation signal was being produced by bursts of pulses rather than a continuous pulse train, we inserted an etalon in the paths of both beams in one arm of the autocorrelator (figure 4) so as to observe the nature of the resulting shift of the multiple spikes. The etalon causes a 20 psec shift in the single-spike autocorrelation signal when it is inserted in one beam, and a 40 psec shift when it is inserted in both beams. Figure 11 illustrates the initial position of the single-spike autocorrelation signal, and the subsequent positions of the signal when the etalon is inserted in one, and then both beams. If the multiple-spike signal is the result of a continuous pulse train, then this signal should not change (shift) when the etalon is inserted. However, we found that the envelope of pulses shifted when we inserted the etalon, thus supporting the hypothesis that the laser produces bursts of pulses.

FIGURE 9

Autocorrelation Signal for a
Finite Pulse Train

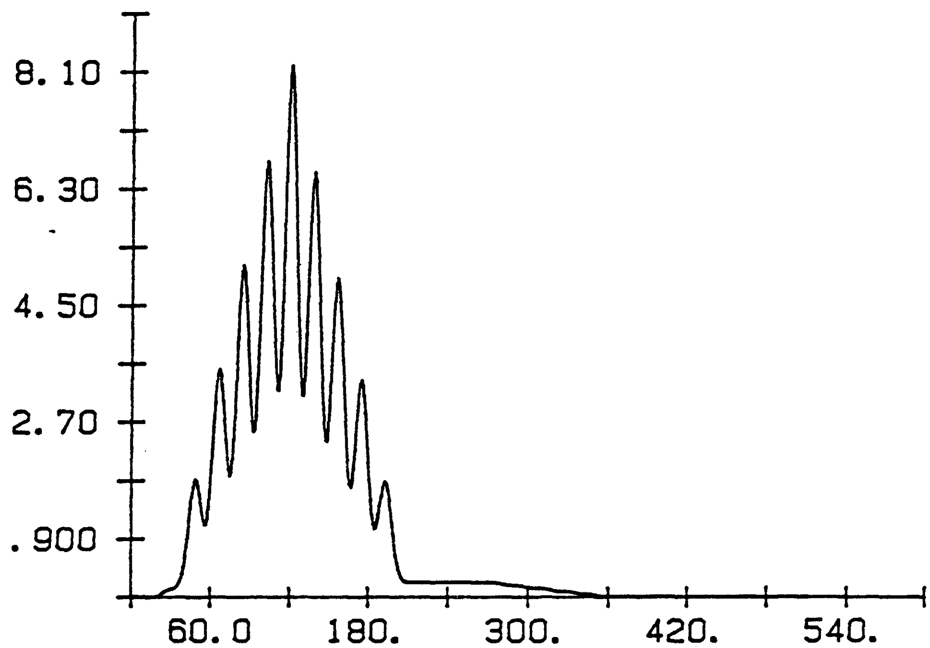

FIGURE 10

Pulse Train Yielding the Autocorrelation
Trace in Figure 9

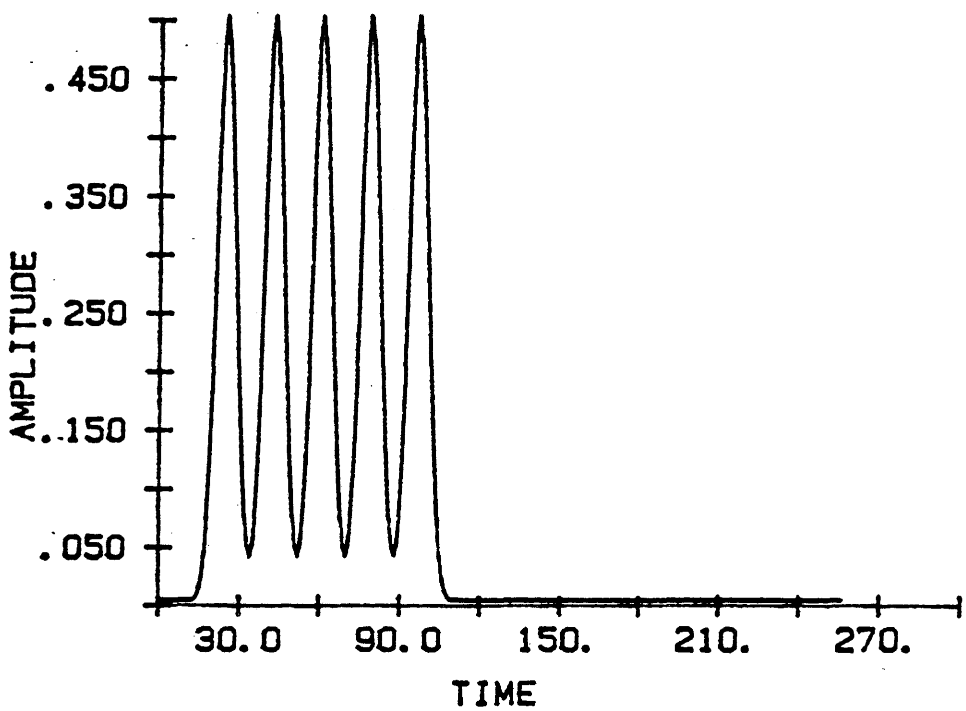

These pulses are Gaussian. The time and amplitude axes are arbitrary, and have significance only with respect to the axes of the autocorrelation function in figure 9.

FIGURE 11

Two 20 Picosecond Shifts of the Single Peak Autocorrelation Trace

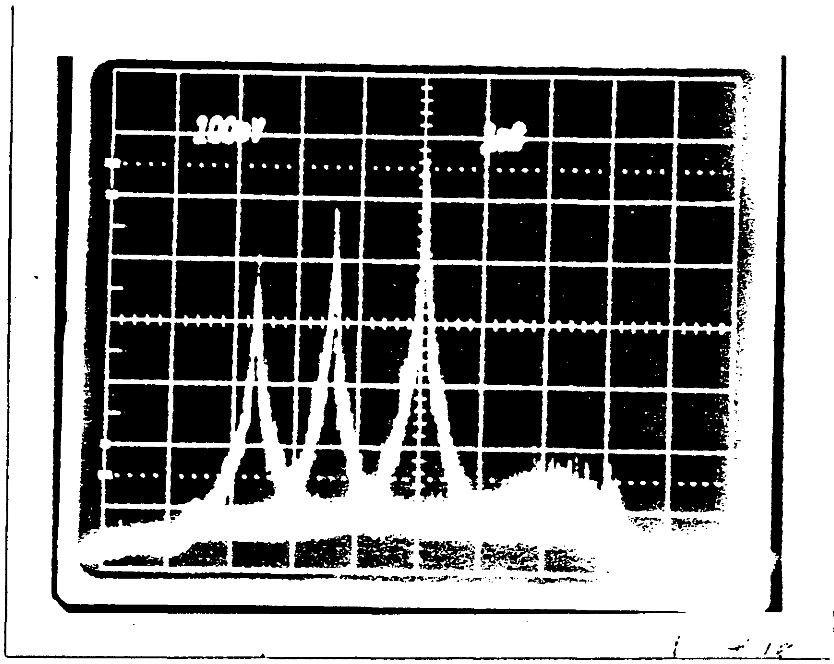

In this photograph, each horizontal division represents 15 psec. The spike on the right is the signal without the etalon inserted. When the beam passes through the etalon, the pulse is delayed by 20 psec. The camera's shutter was left open as the etalon was inserted in the first beam, then both beams.

VII COMPUTER ANALYSIS OF MODE-LOCKING

The computer program MDLCK.INF (appendix C) adds up harmonic waves and plots the pulses resulting from the given number of modes, and the number of times and the magnitude that each mode is frequency shifted. The magnitude of each frequency shift typically was set at or around the free spectral range of the cavity, and the mode spacing is the number of frequency shifts multiplied by the magnitude.

Using this computer model, we wish to support our observations that when either the length or the mode spacing is changed slightly that pulse broadening occurs, and when either of these changes is more substantial then multiple pulses are produced.

To illustrate single-pulse broadening, this program added up the harmonic waves of 10 modes, each being frequency shifted 20 times. The magnitude of each frequency shift is 100 MHz, which corresponds to the free spectral range of a 1.5 meter cavity. The cavity length and the mode spacing were each varied while all other cavity parameters were kept constant. The widths of the pulses produced by the program were measured at the half maximum. This was done by obtaining an array print-out of the calculated pulse. The time scale used was .2 nanoseconds. There are 200 elements in each array, so each element represents 1 psec. The peak value of the array was recorded, and the number of data points in the pulse that were greater than half of the peak value were counted to give the full width, half max.

Table 1 indicates the simultaneous increase of the full width, half max and the decrease in the pulse height as the cavity length is deviated from the value which gives the highest and sharpest pulses. Table 2 and figure 12 show a similar phenomenon occurring as the mode spacing is increased.

The interdependence between the cavity length and the mode spacing is demonstrated by this program when one of these parameters is varied, resulting in the broadening and the decrease in amplitude of the pulse; Then a variation of the other parameter reproduces the optimal pulse. For instance, a pulse having an amplitude of 20,540 and a full width, half maximum of 45 psec is obtained when the mode spacing is 2000.7 MHz and the cavity length is 149.9475 cm.

Beyond a certain deviation in either the cavity length or the mode spacing it becomes difficult to distinguish single pulses because pulse distortion occurs (figures 13 and 14). On the time scale of 25 nsec we observe pulses being produced at a frequency of about one per 5 nsec. The pulses decrease in amplitude while their subsidiary peaks grow as one causes the cavity to move away from the optimal pulsing condition. Figures 15, 16 and 17 illustrate the formation of pulse groups as the mode spacing is increased beyond the range where single pulse production was observed.

A closer inspection (1 nsec time scale) of one of these "pulses" in a pulse group indicates that it is actually a burst of pulses. Figures 18 and 19 illustrate pulse bursts being produced at mode spacings of 2003 MHz and 2005 MHz respectively. It is apparent from these figures that as the mode spacing is deviated from 2000 MHz, the pulse bursts become more spread out. Since the number of pulses in the burst does not change, the spacing between the pulses increases. Figures 20 and 21 are higher resolution (250 psec) plots of figures 18 and 19, respectively. We observe a pulse signal which is very similar to the signal predicted by the program test.pdh. The pulse spacing (7 psec for a mode spacing of 2003 MHz and 12 psec for a mode spacing of 2005 MHz) that is predicted by the program mdlck.inf agrees well with the observed autocorrelation signal.

The pulse height corresponds to the amplitude of the harmonic waves which are mode locked in this computer program. The amplitudes of the waves were all set equal to

1. In addition to being sensitive to variations in the cavity length and the mode spacing, the pulse height is also affected by the total number of harmonic waves that are used in the program (the number of modes multiplied by the number of frequency shifts). For example, figure 20 represents a computation of 200 modes with 20 frequency shifts, and results in pulse heights of around 40,000 and troughs at about zero. Using the same parameters in the program which generated figure 20, except we run it with only 100 modes and 20 frequency shifts, we generate pulses that have the same frequency. However, the pulse heights are below 14,000 and the troughs occur at around 2,000. Thus in addition to affecting the height of the signal, the number of harmonic waves affects the sharpness of the individual pulses.

Figure 22 illustrates pulses occurring at a 4.5 psec interval when the mode spacing is 2001 MHz. This also represents the limit at which distinguishable pulses are observed. At lower values of the mode spacing the troughs and peaks approach the same amplitude (figure 23). Increasing the number of modes allows one to see the pulses that are otherwise indistinguishable. This phenomenon suggests that the high frequency of pulses we observe in the output beam of our laser is the result of the laser's large bandwidth. However, there is still a question as to whether higher frequency pulses are being produced which the autocorrelator is unable to resolve.

TABLE 1

Pulse Characteristics for Increased Cavity Length

Cavity Length	Peak	Full Width, Half Maximum
1.5000 m	20,000	44 psec
1.5005 m	17,835	45 psec
1.5010 m	12,109	50 psec
1.5015 m	6,863	64 psec

Mode spacing was fixed at 2000. MHz

TABLE 2

Pulse Characteristics for Increased Mode Spacing

Mode Spacing	Peak	Full Width, Half Maximum
2000.0 MHz	20,000	44 psec
2000.3 MHz	17,325	45 psec
2000.7 MHz	10,773	49 psec
2001.0 MHz	6,327	56 psec

Cavity length was fixed at 1.5 meters.

FIGURE 12

Broadening and Profile Decline of a Single Pulse due to increased Mode Spacing

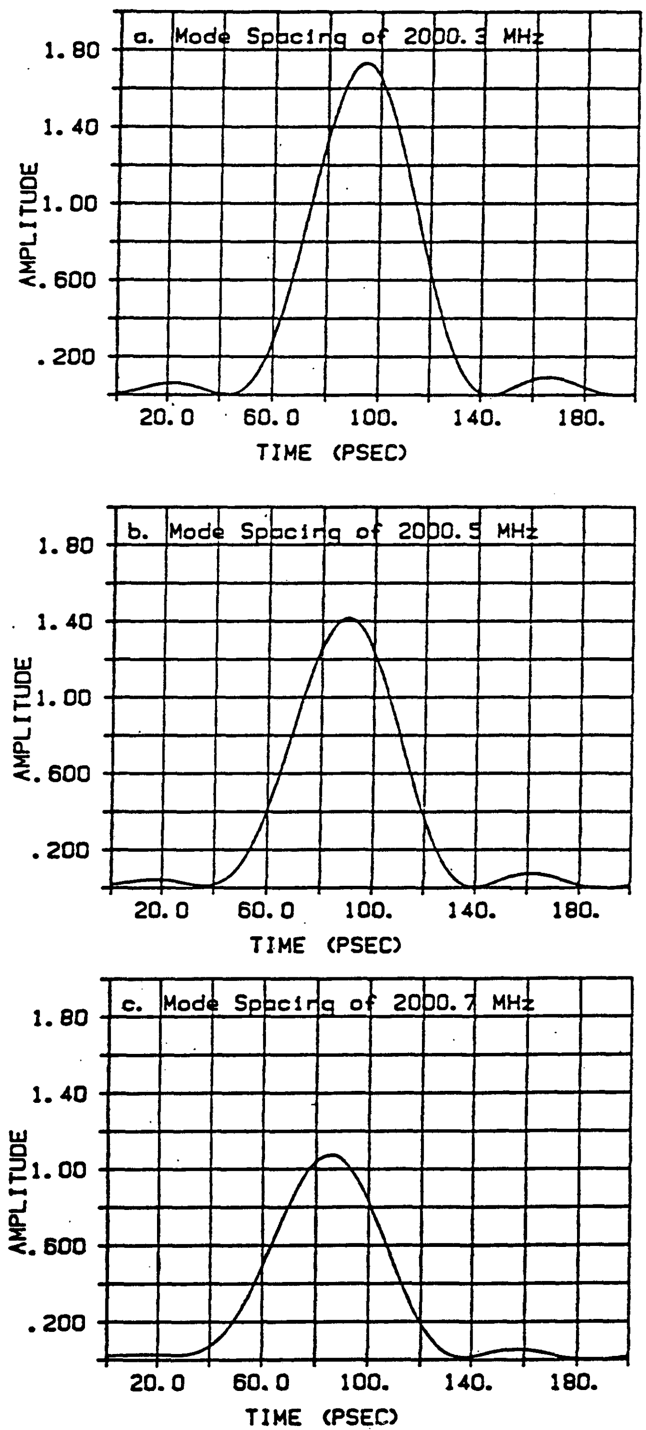

FIGURE 13

Pulse Deformation Occurring as the
Mode Spacing is Increased

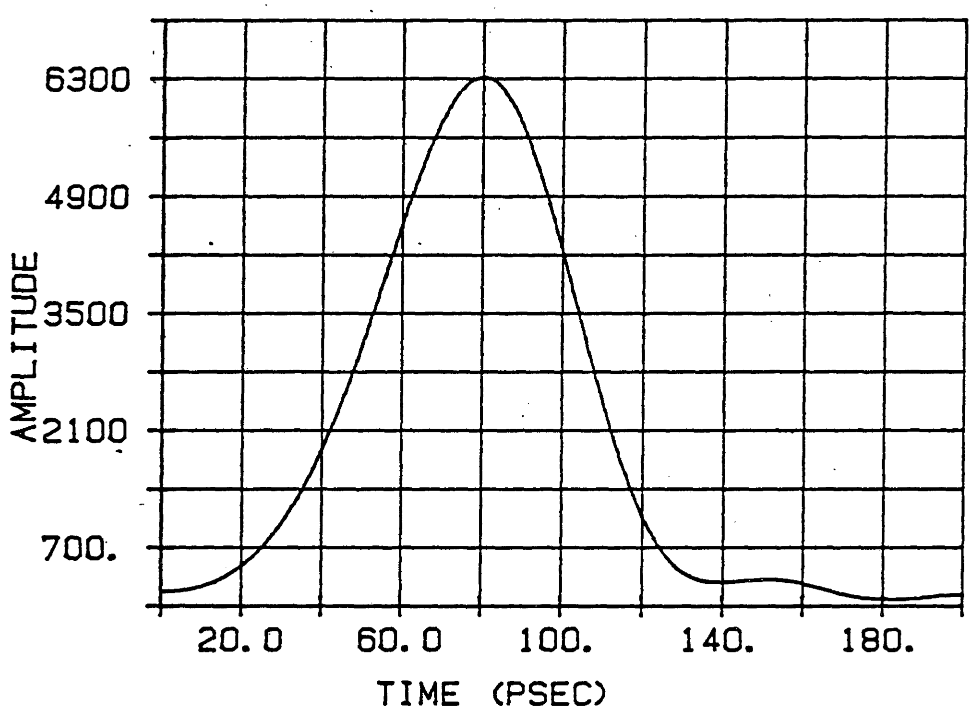

The single pulse autocorrelation signal deforms from its origional Gaussian shape when either the length of the cavity, or the mode spacing is deviated by a significant amount while the other parameter is left unchanged. This plot illustrates deformation beginning to occur when the mode spacing is increased to 2001. MHz and the cavity length is 1.5 meters.

FIGURE 14

Pulse Deformation Occurring as the Cavity Length is Increased

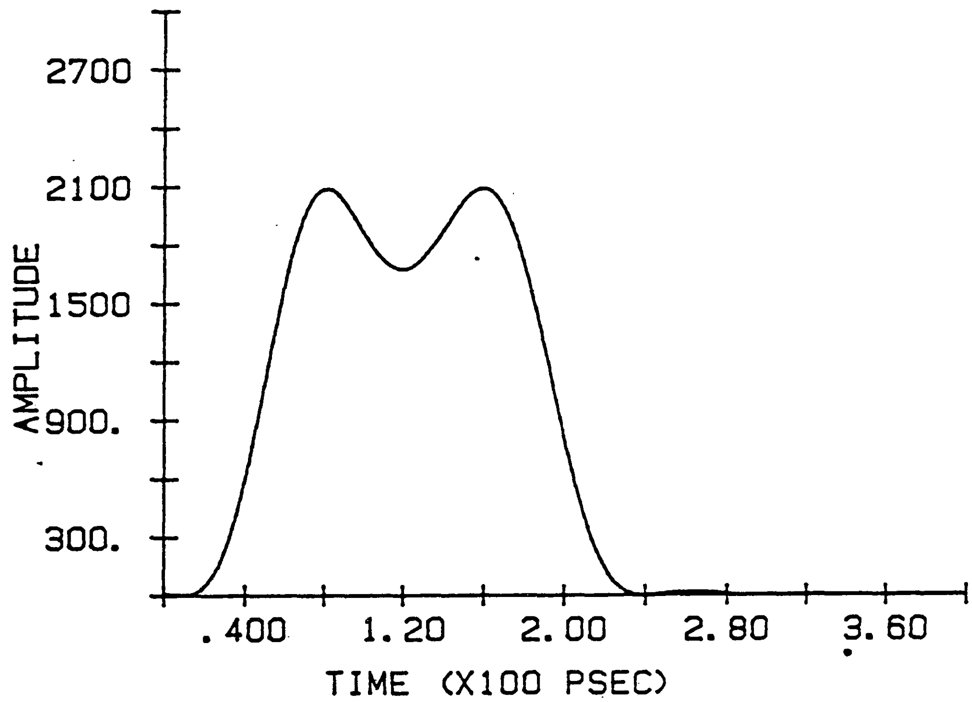

Significant pulse deformation occurring for a cavity length of 1.5025 meters and a mode spacing of 2000. MHz.

FIGURE 15

Optimal Pulse Production

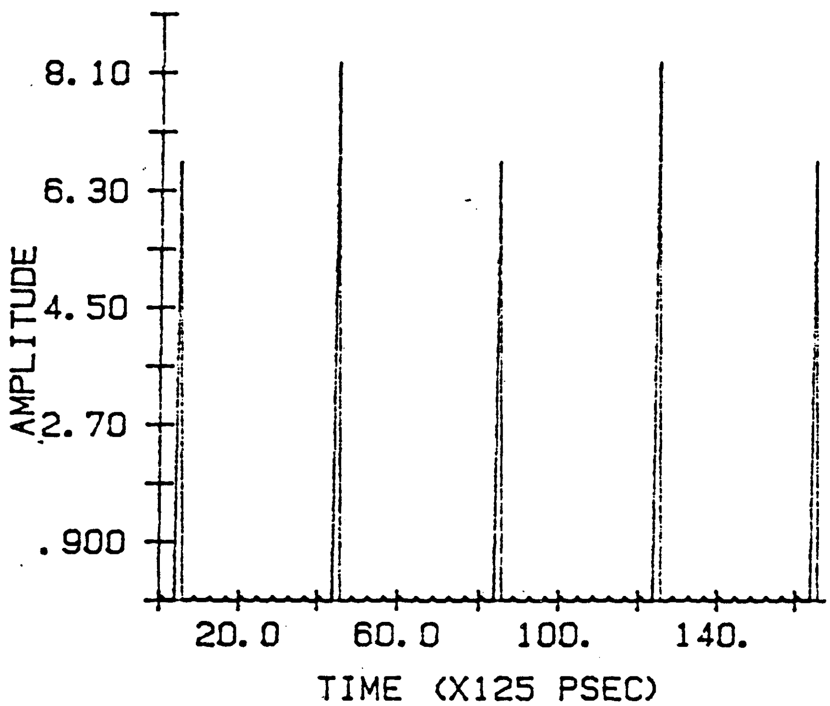

This plot represents pulses produced at the optimum cavity specifications. The cavity length is 1.5 meters and the mode spacing is 2000. MHz. This plot, and all the ones that follow was produced using 200 modes, each having 20 frequency shifts.

FIGURE 16

Multiple Pulses Corresponding to a
Mode Spacing of 2003. MHz

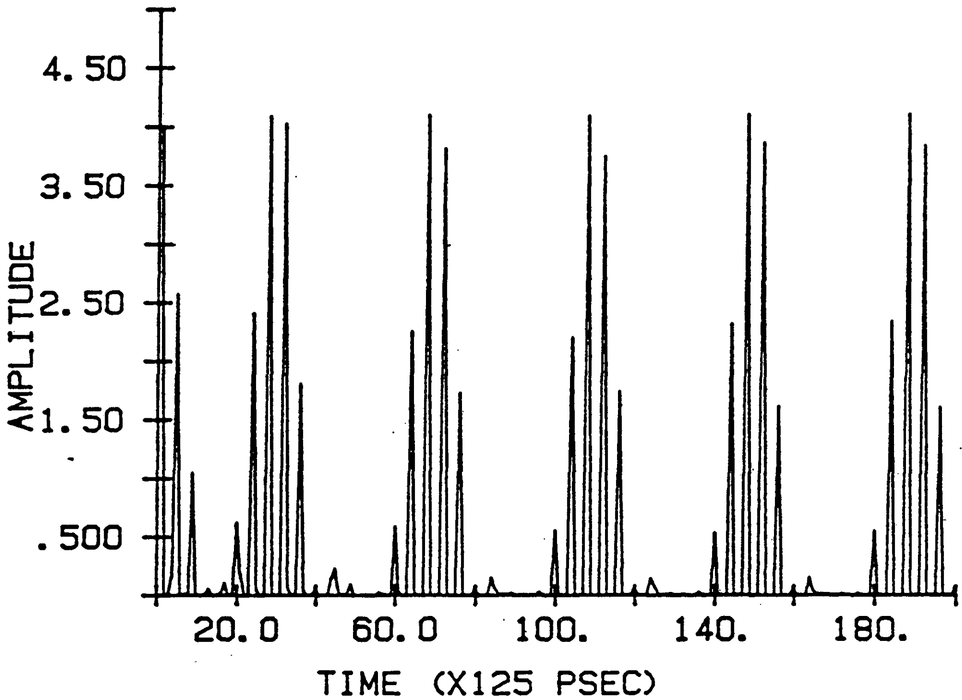

When the mode spacing is increased to 2003. MHz, there are bursts of pulses occurring at about a 5 nsec interval. These pulses are smaller in amplitude than the single pulse signal.

FIGURE 17

Multiple Pulses Corresponding to a
Mode Spacing of 2005. MHz

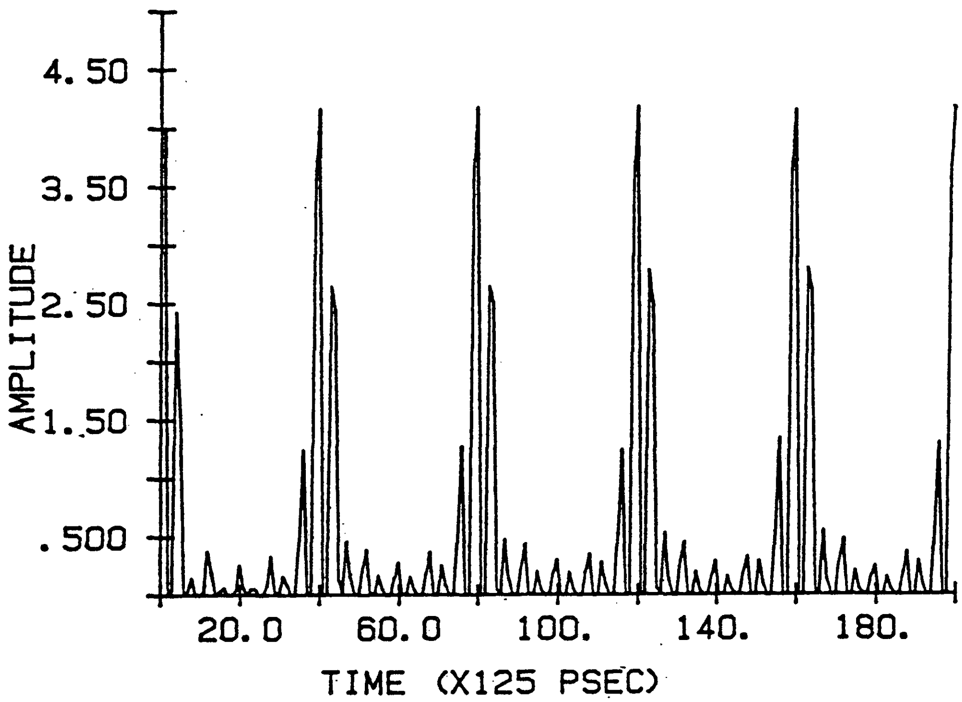

As the mode spacing is increased, we notice that the individual "pulses" in the pulse burst begin to broaden. In actuality, these individual pulses are pulse bursts. This will be illustrated by the high-resolution (1 nsec) plots in figures 18 and 19.

FIGURE 18

High Resolution (1 nsec time scale) Plot of Highest Pulse in Figure 16

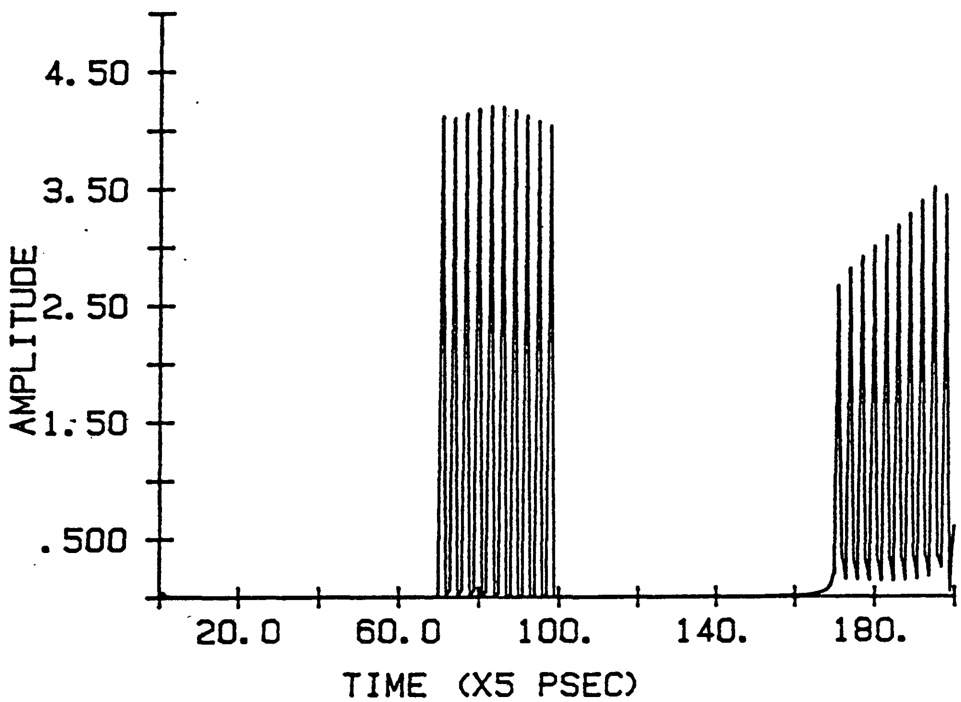

This plot indicates that the individual spikes observed in the previous 2 figures consist of 10 seperate spikes that are very close together. This figure is generated when the mode spacing is 2003. MHz.

FIGURE 19

High Resolution (1 nsec time scale) Plot of Highest Pulse in Figure 17

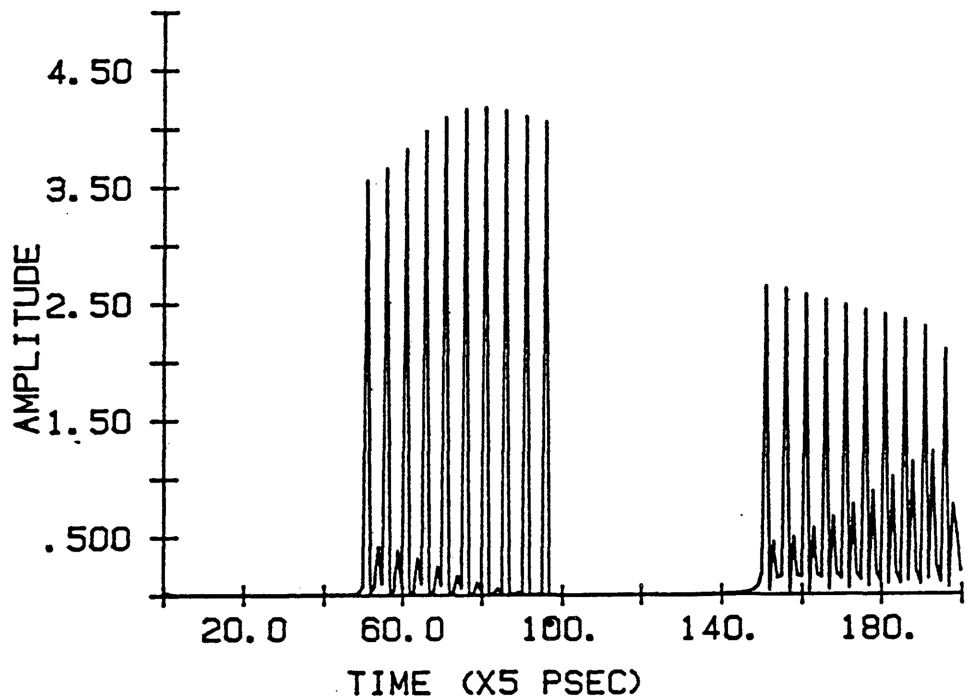

This plot corresponds to a mode spacing of 2005. MHz. We observe that the ten spikes that are observed at this mode spacing are farther apart than the spikes observed in the previous figure (for a mode spacing of 2003. MHz). Thus the pulse burst is broadened as the mode spacing increases.

FIGURE 20

250 Picosecond Time Scale Plot of Pulse Burst in Figure 19

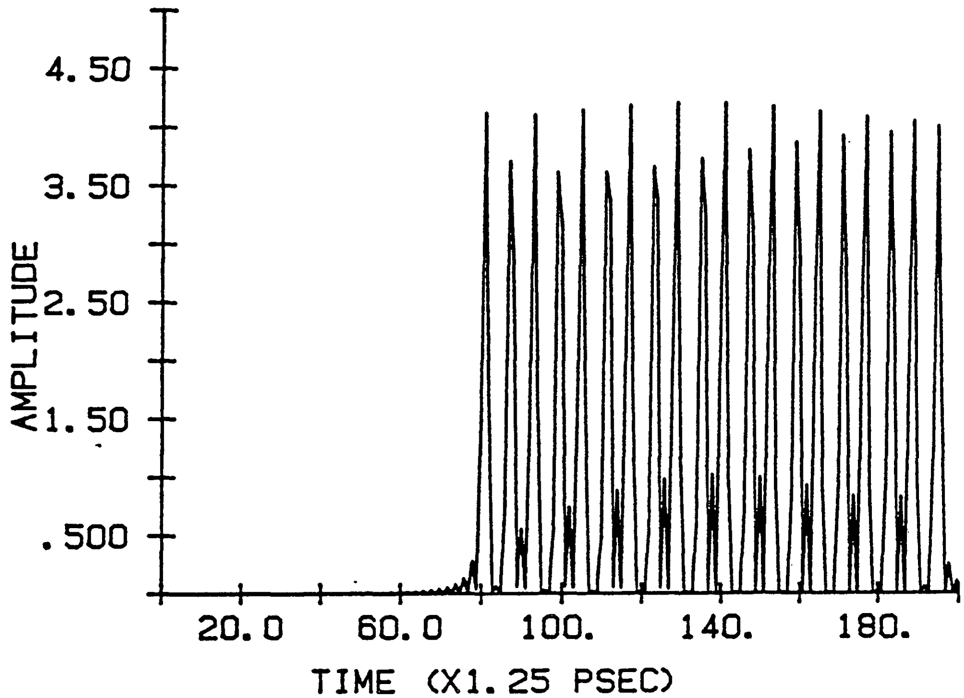

This plot is able to resolve more pulses than the 1 nsec time scale plot, which indicated the presence of only ten pulses. The 250 psec time scale illustrates twenty pulses. Determining the actual number of pulses in a pulse burst requires one to decrease the time scale until one can verify that important information (pulse structure) is not being lost because it occurs within the spacing between data points.

FIGURE 21

250 Picosecond Time Scale Plot of Pulse Burst in Figure 19

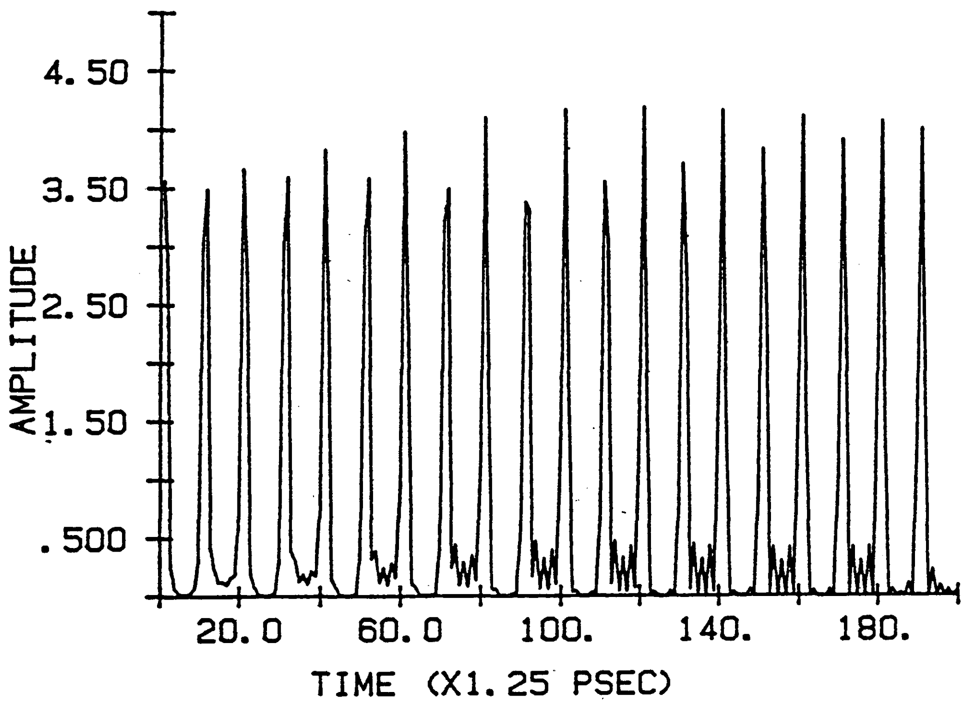

This plot illustrates the individual pulses occurring in a pulse burst when the mode spacing is increased to 2005. MHz. The pulses are farther apart than in the preceeding figure, in which the mode spacing was 2003. MHz. One can determine by looking at this plot that the time scale is small enough such that there are no more significant pulses occurring between those that are plotted.

FIGURE 22

250 Picosecond Time Scale Plot of Pulse Burst for a Mode Spacing of 2001. MHz

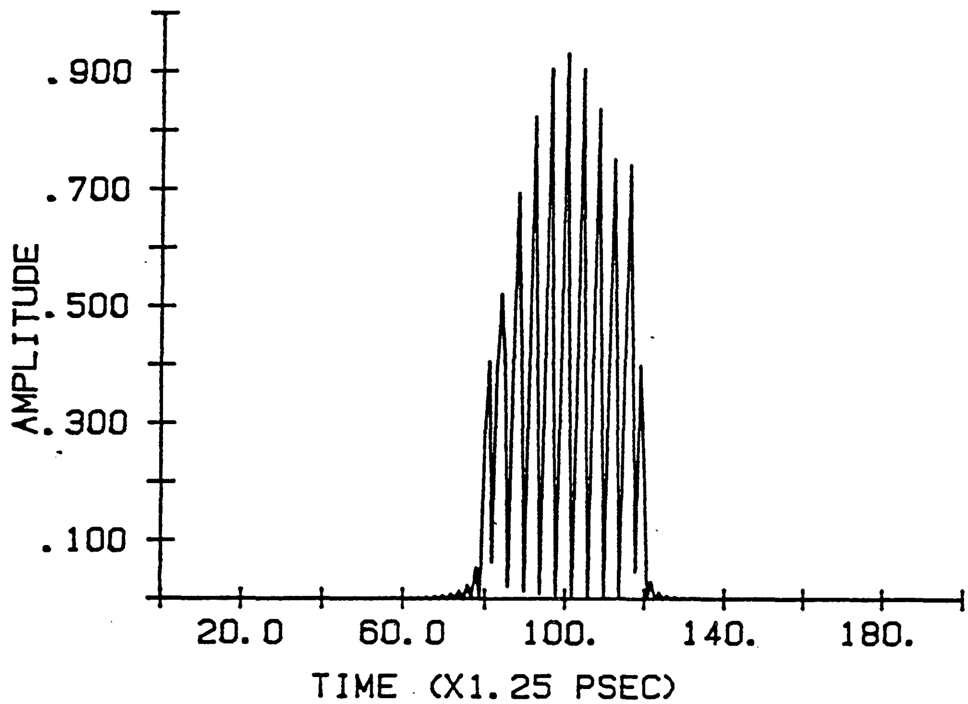

The pulses in this pulse burst are very close together, as would be the expected resulted of the mode spacing being only 1 Mhz away from its optimal value. However, The pulses are too close together to make any comment on the nature of the individual pulses. Thus we must observe this pulse burst on a smaller time scale.

FIGURE 23

100 Picosecond Time Scale Plot of Pulse Burst for a Mode Spacing of 2001. MHz

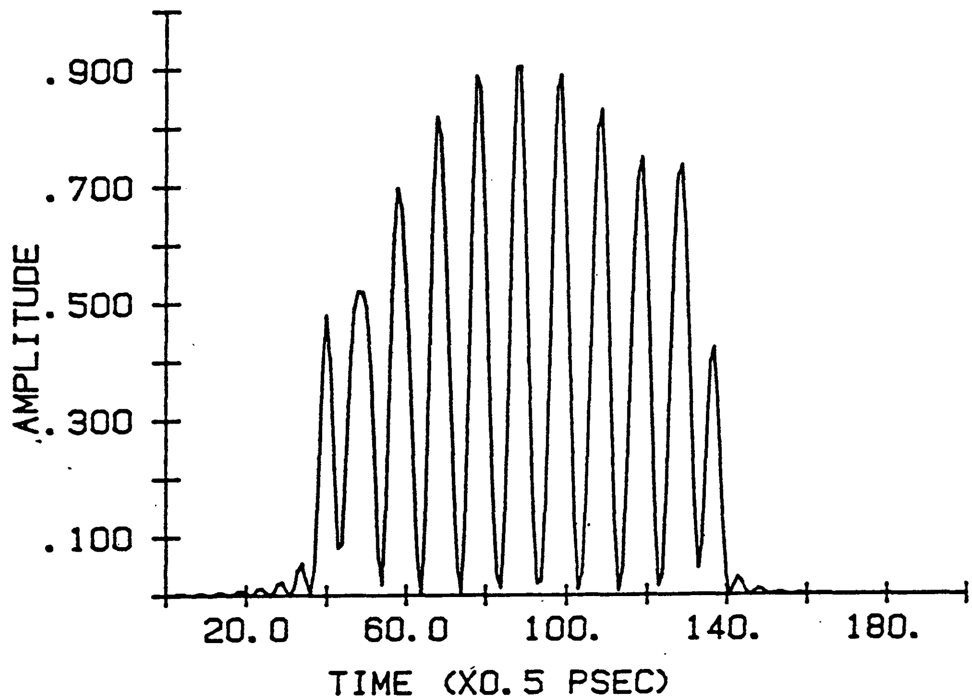

This plot indicates that some of the pulses are starting to fuse together as the mode spacing approaches its optimal value. This is more apparant in the following plot, which illustrates a signal which can no longer be considered as a group of individual pulses.

FIGURE 24

100 Picosecond Time Scale Plot of Deformed Pulse for a Mode Spacing of 2000.9 MHz

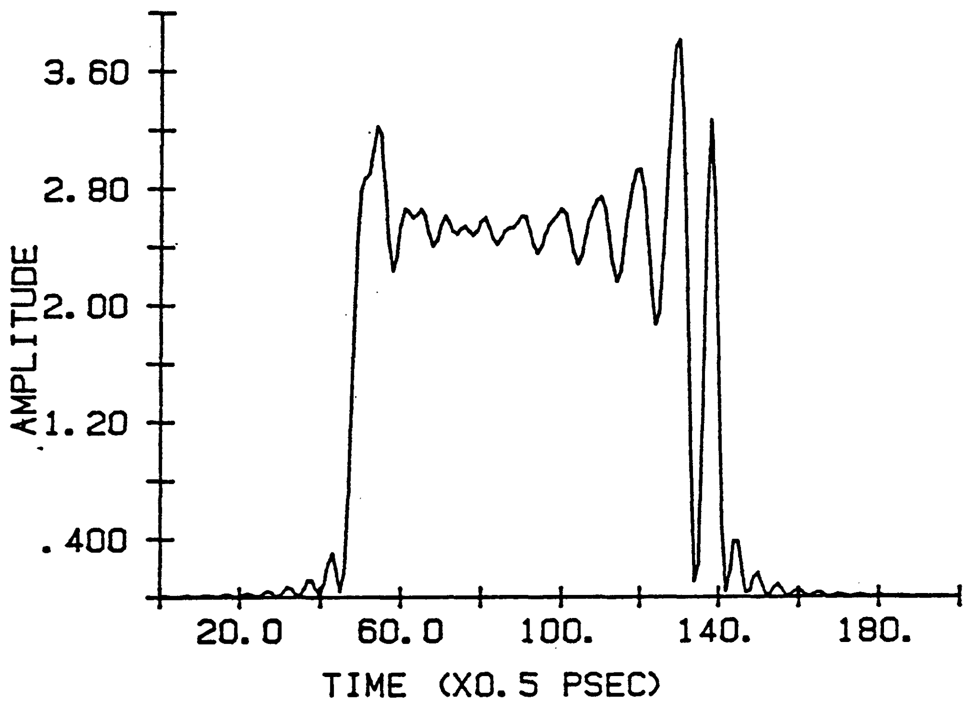

This plot represents the transition between what we identified as single-pulse broadening, and the production of multiple pulses.

REFERENCES

(1) A. Yariv, Quantum Electronics, 2nd ed. (Wiley, New York, 1975) Chapter 9.

(2) J. Verdeyen, Laser Electronics (Prentice-Hall, Englewood Cliffs, N.J., 1981) Chapter 6.

(3) F.V. Kowalski, J.A. Squier, J.T. Pinckney, Appl. Phys. Lett. 50, 711 (1987).

(4) E. Hecht, A. Zajac, Optics, 4th ed. (Addison-Wesley, Reading, Massachusetts, 1979) Chapter 14.4.

APPENDIX A

Stability Calculation Program CAVITY.PAR

```
DP.REAL DIM[ 2 , 2 ] ARRAY TRANSMISSION 0.0 TRANSMISSION :=

1 TRANSMISSION [ 1 , 1 ] :=
1 TRANSMISSION [ 2 , 2 ] :=

DP.REAL DIM[ 2 , 2 ] ARRAY DI 0.0 DI :=
DP.REAL DIM[ 2 , 2 ] ARRAY TL 0.0 TL :=

1 DI [ 1 , 1 ] := 1 DI [ 2 , 2 ] :=
1 TL [ 1 , 1 ] := 1 TL [ 2 , 2 ] :=

STACK.CLEAR

® To calculate distance matrix enter numeric distance
® then type DISTANCE . The transmission matrix is
® automatically updated.

: DISTANCE
DI [ 1 , 2 ] :=
DI TRANSMISSION << * ¶ + >> TRANSMISSION :=
;

® To calculate the matrix for a thin lens enter the focal
® focal then type THINLENS . The transmission matrix is
® automatically updated.

: THINLENS
-1. SWAP /
TL [ 2 , 1 ] :=
TL TRANSMISSION << * ¶ + >> TRANSMISSION :=
;

® The INITIALIZE word is used to reset the transmission
® matrix to the identity matrix so that a new matrix can be
® calculated for a new system.

: S.MIRROR
2. / -1. SWAP /
TL [ 2 , 1 ] :=
TL TRANSMISSION << * ¶ + >> TRANSMISSION :=
;

: INITIALIZE
```

```
0.0 TRANSMISSION :=
1 TRANSMISSION [ 1 , 1 ] :=
1 TRANSMISSION [ 2 , 2 ] :=
;

DP.REAL SCALAR A
DP.REAL SCALAR B
DP.REAL SCALAR C
DP.REAL SCALAR D
DP.REAL SCALAR R
DP.REAL SCALAR W
DP.REAL SCALAR LAMBDA
DP.COMPLEX SCALAR Q

@ The word WAVELENEGTH is used to define the wavelength of
@ light to be used in the calculation. ** Important ** The
@ wavelength command must be used prior to the QUE command
@ or an error will result. Type in a numeric value
@ followed by  wavelength.

: WAVELENGTH
LAMBDA :=
;

@ The QUE command calculates the radius of curvature and
@ the spot size. These values are returned in the real
@ scalar scalar variables R and W . The initial value of R
@ followed by the value W must be entered first, followed
@ by the command QUE .

: SC
1. <=
IF ." STABILITY SATISFIED"
ELSE ." STABILITY NOT SATISFIED"
THEN
;

: QUE
DUP * -1.0 SWAP / LAMBDA * PI /
SWAP 1.0 SWAP / SWAP
Z=X+IY
Q :=

TRANSMISSION [ 1 , 1 ] A :=
TRANSMISSION [ 1 , 2 ] B :=
TRANSMISSION [ 2 , 1 ] C :=
TRANSMISSION [ 2 , 2 ] D :=

D A - 2 B * SWAP /
```

```
R :=

2 LAMBDA * B * PI /
A D + DUP * 4 SWAP - .5 ** / .5 **
W :=
A D + 2 / ABS SC
;
```

APPENDIX B
Autocorrelation Program TEST.PDH

```
REAL SCALAR IT
     SCALAR CENTER 25 CENTER :=
INTEGER SCALAR AA

REAL DIM[ 256 ] ARRAY IN1
     DIM[ 256 ] ARRAY CON
     DIM[ 256 ] ARRAY PULS1
     DIM[ 256 ] ARRAY PULS2

   IN1 []RAMP

   : UNDER.FLOW
   2.5 >= IF
   2.5 CON [ AA ] :=
   THEN
   ;

   : EXE
   1 AA :=
   256 0 DO
   CON [ AA ] UNDER.FLOW
   AA 1 + AA :=
   LOOP
   ;

   : GO
   5 0 DO
   CENTER IN1 - 5 / ABS CON :=

   EXE
   CON DUP * NEG EXP 2 / PULS1 :=
   CENTER 18 + CENTER :=
   PULS1 PULS2 + PULS2 :=
   LOOP
   ;

   GO

   PULS2 PULS2 CONV.APER
   Y.AUTO.PLOT
```

APPENDIX C

Mode-locking Program MDLCK.INF

```
DP.REAL SCALAR N                  @ N = number of peaks
        SCALAR INCREMENT          @ Increment of time on X-axis
        SCALAR T                  @ T = time
        SCALAR T.ROUND.TRIP @ Time of round trip through
                                  @ ring cavity defined by ring
                                  @ ring cavity length divided
                                  @ by the speed of light.
        SCALAR M
        SCALAR INI
        SCALAR N.MODES
        SCALAR RANDOM
        INTEGER SCALAR A
        20 STRING FILENAME
        14 STRING NMFS
        14 STRING C.L
        14 STRING TIME
        40 STRING FREQ
        35 STRING M.S

DP.REAL DIM[ 200 ] ARRAY INTENSITY   @ This array contains
                                     @ the final values for
                                     @ the intensity
DP.COMPLEX DIM[ 200 ] ARRAY MODE.INTENSITY @ Defines the E-
                                 @ field. Taking the square
                                 @ of this quantity yields
                                 @ the intensity.

DP.REAL DIM[ 200 ] ARRAY PHASE
        DIM[ 200 ] ARRAY C.ALPHA
        DIM[ 200 ] ARRAY OFFSET
        DIM[ 200 ] ARRAY FIXED.PHASE
        DIM[ 200 ] ARRAY TYME

0.D PHASE := 0.D C.ALPHA :=
0.D OFFSET := 0.D FIXED.PHASE :=

RAD

: INPUT.PARAMETERS           @ This word is used to prompt the
                             @ user for various input.
```

```
N 0 DO
1.D C.ALPHA [ I 1 + ] :=
A 2005.00E6D * OFFSET [ I 1 + ] :=
LOOP


0.D RANDOM :=

;

: CALCULATE.FIXED.PHASE

0.D  FIXED.PHASE [ 1 ] :=
4.7E14D OFFSET [ 2 ] + 100.00E6D - T.ROUND.TRIP *
FIXED.PHASE [ 2 ] :=
2.4D M :=

N 1 + 3 DO
4.7E14D OFFSET [ I ] + 100.00E6D M * -
T.ROUND.TRIP *
FIXED.PHASE [ I 1 - ] +
FIXED.PHASE [ I ] :=
M 1.D + M :=
LOOP

;

: CALCULATE.INTENSITY                ® This word calculates the
                                     ® intensity using a DO loop
4.2E-9D T :=                         ® *INITIALIZE TIME*
T INI :=
CALCULATE.FIXED.PHASE

201 1 DO
0.D M :=
N 0 DO
4.7E14D OFFSET [ I 1 + ] + 100.00E6D M * -
T *
FIXED.PHASE [ I 1 + ]  +
PHASE [ I 1 + ] :=
M 1.D + M :=
LOOP
PHASE  SUB[ 1 , N ]
2.D DPI * * Z=0+IY RANDOM Z=0+IY +
EXP

C.ALPHA SUB[ 1 , N ] *
[]SUM
```

```
MODE.INTENSITY  [ I ] + MODE.INTENSITY [ I ] :=
T INI - TYME [ I ] :=
T INCREMENT + T :=
LOOP

;

: GRAPH.INTENSITY

TYME INTENSITY XY.AUTO.PLOT            @ Plot the intensity

;

: CREATE.DATA.FILE
  FILE.TEMPLATE
  5 COMMENTS
  REAL DIM[ 200 ] SUBFILE
  END
   CR ." NAME OF DATA FILE ? "
  "INPUT FILENAME ":=
   FILENAME DEFER> FILE.CREATE
   CR ." #MODES/#FREQ SHIFTS ? "
  "INPUT NMFS ":=
   CR ." CAVITY LENGTH ? "
  "INPUT C.L ":=
   CR ." TIME ? "
  "INPUT TIME ":=
   " FREQUENCY SHIFT IS 100. MHZ "
    FREQ ":=
   " MODE SPACING IS 100X FREQ SHIFT "
    M.S ":=
;

: WRITE.DATA.FILE
 FILENAME DEFER> FILE.OPEN
 NMFS 1 >COMMENT
 C.L  2 >COMMENT
 TIME 3 >COMMENT
 FREQ 4 >COMMENT
 M.S  5 >COMMENT
1 SUBFILE INTENSITY ARRAY>FILE
 FILE.CLOSE
;

: EX                          @ Used as an execution word to run
                              @ all of the aforementioned words.
CR ." Number of modes:"
#INPUT N.MODES :=
```

```
@ " Length of ring cavity:"
1.50D 3.0E8D / T.ROUND.TRIP :=

@ " Total time:"
1.E-9D 200.D / INCREMENT :=


CR ." Number of frequency shifts:"
#INPUT N :=
0 A :=
0.D MODE.INTENSITY :=

N.MODES 0 DO
INPUT.PARAMETERS
CALCULATE.INTENSITY
0.D C.ALPHA :=
0.D FIXED.PHASE :=
0.D PHASE :=
A 1 + A :=
LOOP
MODE.INTENSITY CONJ MODE.INTENSITY *
INTENSITY :=
GRAPH.INTENSITY


CREATE.DATA.FILE
WRITE.DATA.FILE

;

: TIME.SCALE

CR ." Total Time:" #INPUT
200.D / INCREMENT :=
CALCULATE.INTENSITY
GRAPH.INTENSITY

;

:  LENGTH

CR ." Length:" #INPUT 300000000.D /
T.ROUND.TRIP :=
CALCULATE.INTENSITY
GRAPH.INTENSITY

;
```